

Simulation of partially spatially coherent laser beam and comparison with field test data for both terrestrial and maritime environments

N. Mosavi^{* a,b}, C. Nelson^c, B. S. Marks^a, B. G. Boone^a, and C. R. Menyuk^b

^aThe Johns Hopkins University Applied Physics Laboratory, 11100 Johns Hopkins Road,
Laurel, MD 20723

^bUniversity of Maryland, Baltimore County, 1000 Hilltop Circle, Baltimore, MD 21250

^cUnited States Naval Academy, 121 Blake Rd, Annapolis, MD 21402

ABSTRACT

We simulate the propagation of both a partially spatially coherent infra-red (IR) and a visible laser beam through a turbulent atmosphere, and we compare the intensity fluctuations produced in the simulation to the intensity fluctuations that are observed in both maritime and terrestrial environments at the US Naval Academy. We focus on the effect of the level of turbulence and the degree of the beam's spatial coherence on the receiver scintillations, and we compare the probability density function (PDF) of the intensity in our simulation to the experimental data. We also investigate the effect of optical beam spreading on the coherent and partially coherent laser beams along the propagation path.

Keywords: Free-space optical communications, Atmospheric turbulence, Aberrations, Monte Carlo simulations

1. INTRODUCTION

Free-space optical communication links support both commercial and military applications due to their high-bandwidth and high directivity, which makes them hard to detect, intercept, and jam. However, these links have some drawbacks as well. A laser beam propagating in free space can undergo significant random intensity fluctuations due to turbulence along the propagation path. A coherent beam (CB) becomes partially coherent when it propagates in atmospheric turbulence, especially in strong turbulence. The theory developed by Banach et al. [1] and recently by Ricklin and Davidson [2] on the use of a spatially partially coherent source beam as applied to atmospheric turbulence for the communication channel shows that it is possible to decrease the receiver scintillations in some cases by reducing the spatial coherence of the beam and thereby improve the bit error ratio (BER).

In this paper, we present simulations of both a partially spatially coherent (PCB) infra-red and a visible laser beam with different degrees of spatial coherence through a turbulent atmosphere. The results have been compared to both maritime and terrestrial field test data that were collected at the US Naval Academy (USNA). We study the effect on the receiver scintillations as the spatial coherence varies, since optimization reduction of the scintillations through control of the degree of spatial coherence can lead to improvements of the BER. Additionally, we compare the probability density function (PDF) of the simulation intensity to what is observed in the field test data, since the PDF of the intensity at the detector is critical for estimation of the fade statistics of an optical signal. At the end, we investigate the effect of the optical beam spread on the coherent and partially spatially coherent beams.

E-mail: *nelofar.mosavi@jhuapl.edu, Telephone: 443-778-3787

2. SIMULATIONS DESCRIPTION

Experimental and simulation implementation of the partially coherent laser light has been accomplished using a spatial light modulator (SLM) for both visible (HeNe) and infra-red (IR) frequencies. A spatial light modulator allows direct control over the phase front of the laser beam. In order to generate a Gaussian Schell model beam (GSM), we developed a MATLAB code to generate a random phase screen using a technique described by Shirai, Korotkova, and Wolf [3]. The initial GSM beam can be written as

$$V_0(\mathbf{r}) = V(\mathbf{r}, z = 0) = \exp\left(-\frac{r^2}{W_0^2}\right) \exp[ig_\phi(r)], \quad (1)$$

where $\mathbf{r} = (x, y)$ is the transverse vector, $r = |\mathbf{r}|$ is the magnitude of the transverse vector, z is the propagation distance, W_0 is the initial beam radius, and $g_\phi(r)$ is a Gaussian-correlated random function and can be written as a convolution integral,

$$g_\phi(r) = \int f_\phi(r - r') R_\phi(r') d^2 r'. \quad (2)$$

The quantity $R_\phi(r)$ is a two-dimensional real-valued random function, that obeys Gaussian statistics with zero mean, while $f_\phi(r)$ is a window function and is given by

$$f_\phi(r) = \exp\left(-\frac{r^2}{\gamma_\phi^2}\right), \quad (3)$$

where γ_ϕ is a positive constant. Figure 1 shows sample phase screens with different values of γ_ϕ^2 that were used in our simulations and experiments.

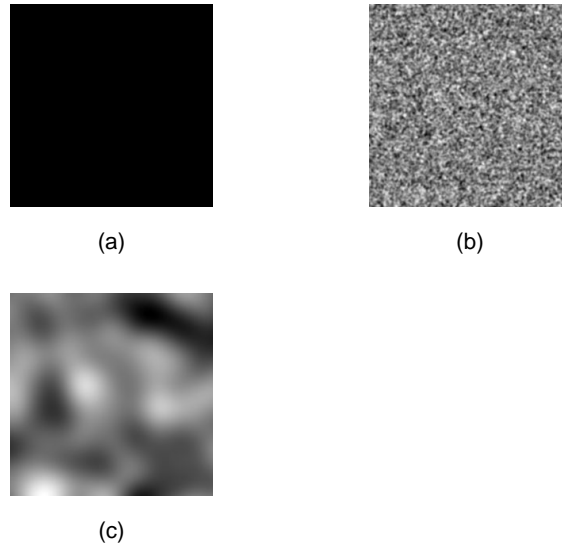


Figure 1. (a) $\gamma_\phi^2 = \infty$ (coherent), (b) $\gamma_\phi^2 = 1$ (strong diffuser), (c) $\gamma_\phi^2 = 16$

In order to model the propagation of a GSM beam through turbulence, we first write the paraxial wave equation [4],

$$2ik \frac{\partial V(\mathbf{R})}{\partial z} + \nabla_T^2 V(\mathbf{R}) + 2k^2 n_1(\mathbf{R}) V(\mathbf{R}) = 0, \quad (4)$$

where $\mathbf{R} = (\mathbf{r}, z)$ is the position vector, ∇_T^2 is the transverse Laplacian operator, k is the wavenumber, $V(\mathbf{R})$ is the envelope of the electric field of the GSM beam, and $n_1(\mathbf{R})$ is the randomly fluctuating portion of the

atmosphere's refractive index. The turbulent contribution to the evolution over a length Δz is given by

$$V(\mathbf{r}, z + \Delta z) = V(\mathbf{r}, z) \exp \left[ik \int_0^{\Delta z} dz' n_1(\mathbf{r}, z') \right]. \quad (5)$$

We then write the first two statistical moments of $\theta \equiv k \int_0^{\Delta z} dz' n_1(\mathbf{r}, z')$ as

$$\langle \theta \rangle = k \int_0^{\Delta z} dz' \langle n_1(\mathbf{r}, z') \rangle = 0 \quad (6)$$

and

$$\langle \theta^2 \rangle = k^2 \int_0^{\Delta z} dz' \int_0^{\Delta z} dz'' \langle n_1(\mathbf{r}, z') n_1(\mathbf{r}, z'') \rangle. \quad (7)$$

We use the method of randomly varying phase screens, combined with the split-step method [5], to calculate $V(\mathbf{r}, z)$ for a particular realization. We use the von Karman-Tatarski spectrum to calculate the phase screens. In order to find the beam radius we use the moment method as described by Feizulin and Kravtsov [6] and by Gbur and Wolf [7]. We calculated the beam radius squared $\langle W^2 \rangle_{\text{MC}} = 2 \langle r^2 \rangle_{\text{MC}}$ using the Monte Carlo technique, where $\langle \cdot \rangle_{\text{MC}}$ denotes the ensemble average of the Monte Carlo realizations [8]. We have

$$\langle W^2 \rangle_{\text{MC}} = 2 \langle r^2 \rangle_{\text{MC}} = 2 \frac{\int \int_{-\infty}^{\infty} d^2r r^2 \langle I(\mathbf{r}, z) \rangle}{\int \int_{-\infty}^{\infty} d^2r \langle I(\mathbf{r}, z) \rangle}, \quad (8)$$

where $I(\mathbf{r}, z) = |V(\mathbf{r}, z)|^2$ is the irradiance of the beam.

3. FIELD TEST DESCRIPTION

For the USNA field test, both an IR (1550 nm) and an HeNe (632.8 nm) laser were used. The IR laser beam was used over land with a 180 m propagation distance, and the HeNe laser was used over water with a 314 m propagation distance. In both experiments, the laser beam was vertically polarized, went through a beam expander (IR and visible), was reflected from a 7.68 mm \times 7.68 mm SLM (IR and visible), and then propagated through the atmosphere to a target receiver. At the receiver an amplified photodetector and data acquisition system were used to collect data at 10,000 samples/second. Each data run was approximately two minutes in duration. A scintillometer was used to estimate the value of refractive-index structure parameter, C_n^2 , over the propagation path for both field tests. We measured $C_n^2 = 1 \times 10^{-14} \text{ m}^{-2/3}$ for the 314 m path over a creek. We believe that the scintillometer may have been misaligned during the 180 m terrestrial test, and we therefore estimated $C_n^2 = 1 \times 10^{-15} \text{ m}^{-2/3}$ based on previous measurements. For more details on the field test data, see Ref. 9.

4. FIELD TEST DATA VS. SIMULATIONS

Figures 2 and 3 show a comparison of the Monte Carlo simulations with the field test data at a propagation distance of 314 m for the HeNe laser and 180 m for IR beam with lognormal PDF distributions. In order to match the probability distribution of the simulations with the field test data, we used $C_n^2 = 1 \times 10^{-13} \text{ m}^{-2/3}$ for IR beam, and we used $C_n^2 = 8 \times 10^{-15} \text{ m}^{-2/3}$ for HeNe beam. These values differ somewhat from the path average values that were estimated at the time of the experiments, but are within the error ranges of these estimates. These estimates were rough, and, in fact, comparison to Monte Carlo simulations like ours is an effective means of deducing the actual values. With weak turbulence fluctuations, the lognormal PDF should agree well with both our simulations and experiments. The fluctuation regime is defined by the Rytov variance [4],

$$\sigma_R^2 = 1.23 C_n^2 k^{7/6} z^{11/6}. \quad (9)$$

The weak fluctuation regime corresponds to $\sigma_R^2 < 1$, while the moderate-to-strong fluctuation regime corresponds to $\sigma_R^2 > 1$. For the HeNe beam propagation, the Rytov variance is $\sigma_R^2 = 0.05$ and for the IR beam propagation, it is $\sigma_R^2 = 0.08$; so, our experiments are in the weak fluctuation regime.

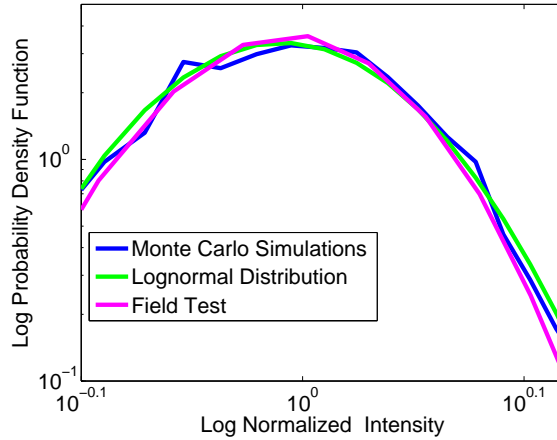


Figure 2. Comparison of the Monte Carlo simulations and the field test with a degree of coherence $\gamma_\phi^2 = 2$ to the lognormal PDF model for the IR beam at a propagation distance of 180 m.

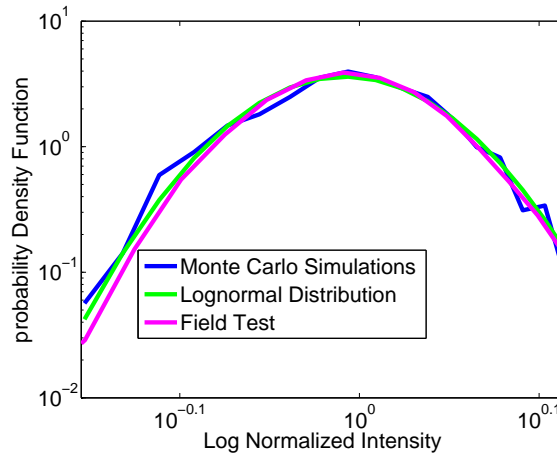


Figure 3. Comparison of the Monte Carlo simulations and the field test with a degree of coherence $\gamma_\phi^2 = 2$ to the lognormal PDF model for the HeNe beam at a propagation distance of 314 m.

Tables 1 and 2 show a comparison of the scintillation index for varying spatial coherence from fully coherent to nearly incoherent that we obtained from Monte Carlo simulations and from the experiments for the IR beam over 180 m and the HeNe beam over 314 m. The scintillation index is the irradiance variance scaled by the square of the mean irradiance [4],

$$\sigma_I^2(\mathbf{r}, z) = \frac{\langle I^2(\mathbf{r}, z) \rangle}{\langle I(\mathbf{r}, z) \rangle^2} - 1, \quad (10)$$

where the irradiance is equal to mutual coherence function, $\langle I(\mathbf{r}, z) \rangle = \Gamma_2(\mathbf{r}, \mathbf{r}, z)$, and the second moment of the irradiance is the fourth-order coherence function, $\langle I^2(\mathbf{r}, z) \rangle = \Gamma_4(\mathbf{r}, \mathbf{r}, \mathbf{r}, \mathbf{r}, z)$.

For the IR beam simulations, the strongest diffusers, which corresponds to $\gamma_\phi^2 = 1$ through 8, have higher scintillation indices than the fully coherent beam. The scintillation index is lower than the coherent beam for the partially spatially coherent beam with $\gamma_\phi^2 = 16$ and $\gamma_\phi^2 = 128$, which are “possible sweet spot” of the scintillation indices. Values of γ_ϕ^2 at which the scintillation index is less than its value for the coherent beam have been referred to as “possible sweet spots” [9]. By “possible” we mean that the value of γ_ϕ^2 at which a “sweet spot” occurs depend on C_n^2 and z . For the IR beam experiment, we find a possible sweet spot at $\gamma_\phi^2 = 32$. Table 2 shows the scintillation results for the HeNe beam. The simulation results indicate that $\gamma_\phi^2 = 16$ is a possible sweet spot. The HeNe experimental results indicate that all values of γ_ϕ^2 in the range of $1 \leq \gamma_\phi^2 \leq 64$ are possible sweet spots. The simulations are in the reasonable agreement with the experiments, given experimental uncertainties

γ_ϕ^2	<i>Scintillation</i>	
	Simulations	Experiment
Black (coherent)	0.0114	0.0063
1 (Strong diffuser)	0.0132	0.0110
2	0.0170	0.0121
4	0.0136	0.0105
8	0.0120	0.0102
16	<i>0.0110</i>	0.0079
32	0.0114	<i>0.0057</i>
64	0.0115	0.0077
128 (weak diffuser)	<i>0.0113</i>	0.0074

Table 1. Scintillation Indices for the IR laser beam at a propagation distance of 180 m with a varying spatial coherence for both field test data [9] and simulations. The blue italics indicate possible scintillation index sweet spots.

γ_ϕ^2	<i>Scintillation</i>	
	Simulations	Experiment
Black (coherent)	0.0076	0.0119
1 (Strong diffuser)	0.0090	<i>0.0101</i>
2	0.0124	<i>0.0115</i>
4	0.0093	<i>0.0107</i>
8	0.0080	<i>0.0095</i>
16	<i>0.0073</i>	<i>0.0107</i>
32	0.0076	<i>0.0094</i>
64	0.0076	<i>0.0095</i>
128 (weak diffuser)	0.0075	0.0122

Table 2. Scintillation Indices for the HeNe laser beam at a propagation distance of 314 m with varying spatial coherence for both field test data [9] and simulations. The blue italics indicate possible scintillation index sweet spots.

in C_n^2 . Both simulation and experiment indicate that possible sweet spots exist for both the IR and HeNe laser beams. We attribute the differences in the scintillation indices between the field test data and the simulations primarily to errors in the estimates of the C_n^2 in the experiment, but we also note that the photodetector had an aperture of 2.45 cm at the test setup, while the simulation used point measurement of the center intensity profile in order to save computation time.

In Figs. 4(a) and 4(b), we show the beam spreading for the HeNe beam both with and without turbulence for the coherent beam and partially coherent beam in the case $\gamma_\phi^2 = 16$. As expected, the partially coherent beam spreads more both with turbulence and without turbulence than the coherent beam. In order to investigate the effect of beam spreading due only to turbulence, we look at the relative beam spread, which is the difference between the beam spread without turbulence and turbulence for each case. The relative beam spread for both the HeNe beam and the IR beam is presented in Figs. 5(a) and 5(b). The results show that relative beam spread is lower for partially coherent beams than it is for coherent beams. We conclude that partially coherent beams are less distorted by atmospheric turbulence than is a coherent beam in cases where the scintillation indices of the partially coherent beams are smaller than is the scintillation index of a coherent beam.

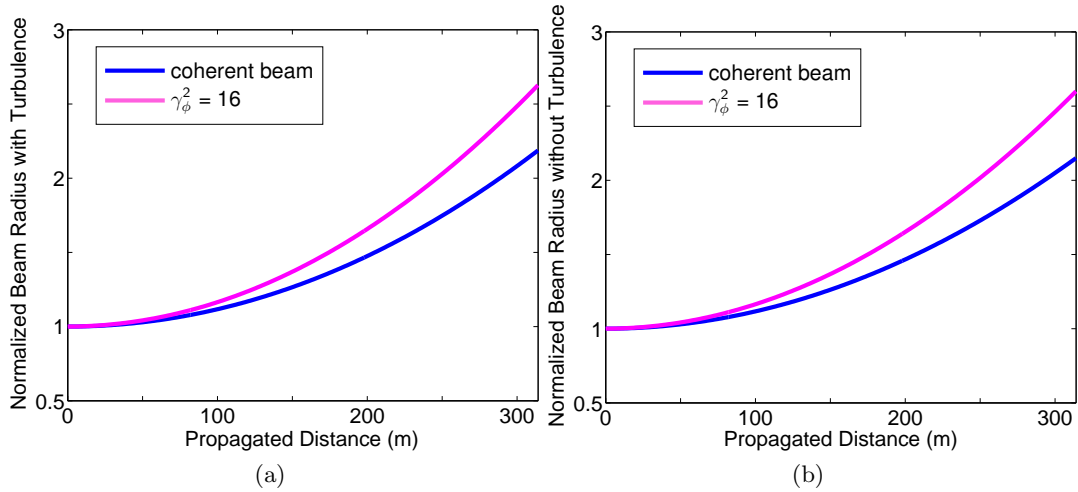


Figure 4. The beam spreading for the HeNe beam for a coherent and a partially coherent beam with $\gamma_\phi^2 = 16$ at a propagation distance of 314 m. (a) with turbulence and (b) without turbulence.

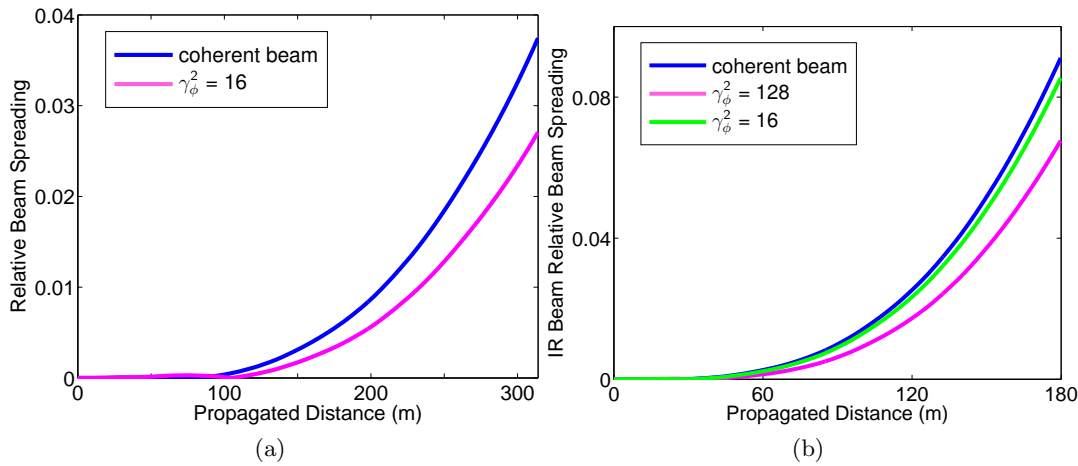


Figure 5. Relative beam spreading for a coherent and a partially coherent beams: (a) HeNe beam at a propagation distance of 314 m and (b) IR beam at a propagation distance of 180 m.

5. CONCLUSION

We present simulations of partially spatially coherent infra-red and visible (HeNe) laser beams with different degrees of spatial coherence through a turbulent atmosphere. The results have been compared to both maritime and terrestrial field test data that were collected at the US Naval Academy. We compared the probability density function of the intensity in the simulation to what was observed in the field test data. The simulations predict a lognormal probability distribution function in agreement with experiments. We studied the effect of varying spatial coherence on the receiver scintillation index. We have shown that the scintillation index has possible sweet spots associated with specific degrees of partial spatial coherence of the laser beam, and which depend on the propagation distance and atmospheric parameters. We obtained good agreement between the scintillation index that is found experimentally and the scintillation index that is calculated in our simulations. Finally, we investigated beam spreading for both coherent and partially spatially coherent beams. We showed that partially coherent beams whose scintillation indices are lower than the index of a coherent beam are also less distorted by atmospheric turbulence.

6. ACKNOWLEDGMENTS

This work was supported by the Johns Hopkins University Applied Physics Laboratory through an IRAD grant. The authors would like to thank R. Sova for encouragement and support.

REFERENCES

1. V. A. Banach, V. M. Buldakov, and V. L. Mironov, "Intensity fluctuations of a partially coherent light beam in a turbulent atmosphere," *Opt. Spektrosk.* **54**, 1054–1059 (1983).
2. J. C. Ricklin, and F. M. Davidson, "Atmospheric optical communication with a Gaussian Schell beam," *J. Opt. Soc. Am. A* **20**, 856–866 (2003).
3. T. Shirai, O. Korotkova, and E. Wolf, "A method of generating electromagnetic Gaussian Schell-model beams," *J. Opt. A: Pure Appl. Opt.* **7**, 232–237 (2005).
4. L. C. Andrews and R. L Phillips, *Laser Beam Propagation Through Random Media* (SPIE Press, Bellingham, WA, 2005).
5. T. Poon and T. Kim, *Engineering Optics With Matlab* (World Scientific Publ., 2006).
6. Z. I. Feizulin and Yu. A. Kravtsov, "Broadening of laser beam in a turbulent medium," *Radiophys. Quantum Electron.* **10**, 33–35 (1967).
7. G. Gbur and E. Wolf, "Spreading of partially coherent beams in random media," *J. Opt. Soc. Am.* **19**, 1592–1598 (2002).
8. N. Mosavi, B. S. Marks, B. G. Boone, and C. R. Menyuk, "Optical beam spreading in the presence of both atmospheric turbulence and quartic aberration," in *Free-Space Laser Communication and Atmospheric Propagation XXVI*, H. Hemmati and D. M. Boroson, eds., Proc. SPIE **8971**, 897102 (2014).
9. C. Nelson, S. Avramov-Zamurovica, O. Korotkovab, R. Malek-Madania, R. Sovac, and F. Davidson, "Measurements of partially spatially coherent laser beam intensity fluctuations propagating through a hot-air turbulence emulator and comparison with both terrestrial and maritime environments," in *Free-Space Laser Communication and Atmospheric Propagation XXV*, H. Hemmati and D. M. Boroson, eds., Proc. SPIE **8610**, 86100T (2013).